Title
Development of a combined ultrasound and photoacoustic endoscopic probe

ISBN
9780819484307

Authors
Wei, Wei
Li, Xiang
Zhou, Qifa
et al.

Publication Date
2011-02-10

DOI
10.1117/12.874505

Development of a combined ultrasound and photoacoustic endoscopic probe

Wei Wei[a] , Xiang Li[b], Qifa Zhou[b], K. Kirk Shung[b] , and Zhongping Chen[a]
[a]Beckman Laser Institute, University of California Irvine, Irvine CA 92612-1475
[b]NIH Transducer Resource Center and Department of Biomedical Engineering, University of Southern California

ABSTRACT

For *in vivo* medical applications, endoscopy shows great potential for its minimally invasive manner, flexibility and close-up imaging characteristic. A miniaturized imaging probe combining ultrasound and photoacoustic endoscopy has been developed. The output of a 532-nm pulse laser was coupled into and delivered to the probe by a 200-micron-core multimode fiber. A 40 MHz ring shape ultrasound transducer was fabricated to receive pulse echo ultrasound and photoacoustic signals as well. The light-guiding optical fiber, the ring ultrasound transducer, and a mirror-based reflective material for the coaxial laser beam and ultrasound signal were integrated into the probe with a final packaged diameter of 2.5 mm. The performance of the probe was tested by imaging a graphite rod. The imaging ability of this dual-modality system was demonstrated by imaging the cross section of a rabbit aorta.

1. ITRODUCTION

Photoacoustic imaging has been develeoped as a hybird imaging technique that shows great potential for *in vivo* medical application[1 2 3 4]. Due to the electromagnetic absorption of tissues, broadband acoustic waves can be excited by using a nanosecond pulse laser. The photoacoustic wave can be detected and spatially resolved by an ultrasound transducer. Consequently, the advantages of high ultrasonic resolution and strong optical absorption contrast are combined in this imaging modality.

In the past few years, photoacoustic computed tomography has succeeded in detecting brain lesion and monitoring hemodynamics[1 5 6]. Meanwhile, photoacoustic microscopy can achieve tens of micron resolution beyond the penetration limit at transport mean free path[7 8]. However, the photoacoustic signal from deeper regions of an organ is insufficient in some cases. Photoacoustic endoscopy has the advantages of minimally invasive manner, flexibility and close-up imaging characteristic. A photoacoustic endoscopic probe with diameter of 4.2 mm and length of 48 mm was reported by Joon-Mo Yang [9 10]et al.. On the other hand, endoscopic ultrasonography is the most commonly used technique in clinics, especially when used in a patient's upper digestive tract and respiratory system. Nevertheless, ultrasonography cannot achieve the specificity and contrast requirement sometimes, because of its imaging mechanism. Therefore, based on the matured ultrasound endoscopy, a combined system with both ultrasound and photoacoustic imaging ability was developed. S. Sethuraman et al[11] reported the combined intravascular ultrasound and photoacoustic imaging system. However, the external light illumination is not feasible in some in vivo experiment.

In this paper, we present a combined ultrasound and photoacoustic probe by introducing an optical delivery fiber and sharing the same ring shape ultrasound transducer for detection. The fiber runs through the center of the ring transducer. The micro rod mirror was used to reflect laser beam, ultrasonic and photoacoustic signal. Based on this design, we can acquire co-registered endoscopic imaging automatically because of coaxial nature of the ultrasonic beam and the laser beam.

Endoscopic Microscopy VI, edited by Guillermo J. Tearney, Thomas D. Wang, Proc. of SPIE Vol. 7893, 789317 · © 2011 SPIE · CCC code: 1605-7422/11/$18 · doi: 10.1117/12.874505

2. MATERIALS AND METHOD

2.1 The ultrasound-based hybrid imaging system

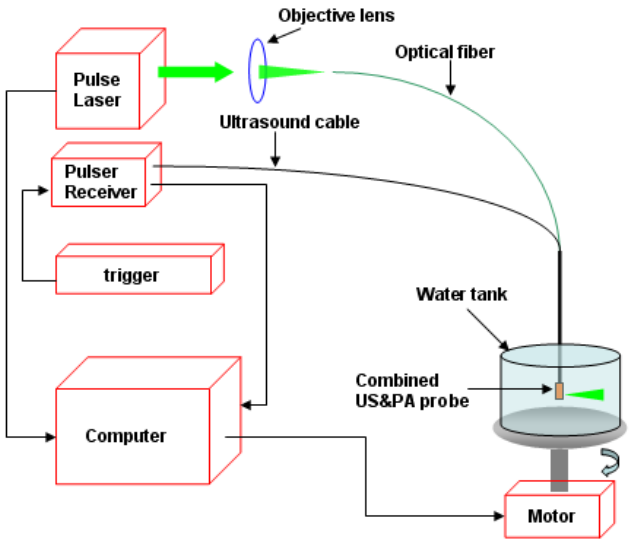

Figure 1. The prototype of the hybrid ultrasonic and photoacoustic imaging system.

In our ultrasound based hybrid imaging system(Fig.1), the pulsed Q-switched Nd: YAG laser (532 nm wavelength, 3-5 ns pulse width, 10 Hz repetition rate, Contimuum, Inc.) was used as an excitation source. The free space laser beam was coupled into a 200-micron-core multimode fiber by an objective lens. The home-made 40 MHz ring shape ultrasonic transducer and light delivery medium were combined together. The combined probe was inserted into the lumen of a phantom or a tissue, and the target area was illuminated internally. The tissue or the phantom was immersed and fixed in a water tank. The circumferential scanning (B-scan) is accomplished by rotating the tank which was driven by a stepping motor. The pulser and receiver unit (Olympus NDT, Inc., Kennewick, WA) was used to generate ultrasound pulse, meanwhile, receive both ultrasonic echo and photoacoustic wave. For each circular B-scan, 1000 time-resolved photoacoustic signals (A-lines), as well as the ultrasonic echoes are recorded. The received echo and photoacoustic signal were then digitized by a 12-bit data acquisition board (Gage Applied Technologies, Lockport, IL) with sampling rate of 200 MHz.

2.2 Combined ultrasound and photoacoustic probe

Fig. 2(a) is the schematic of combined ultrasound and photoacoustic probe. The 200-micron-core multimode optical fiber was inserted through the central hollow region of the 40 MHz ring shape ultrasound transducer. The coaxial optical laser beam and ultrasound beam was steered by the same customized micro rod mirror (platinum coating, 2.0 mm diameter, 4 mm length, with the reflective surface angled at 45 degrees to the probe's axis). Also, the excited photoacoustic wave was reflected by the mirror and detected by the ultrasound transducer. Fig. 2(b) shows the ring shape ultrasound transducer with 2.4 mm outer diameter and 0.6mm inner diameter. The whole combined probe was packaged in a polyimide tube with a final packaged diameter of 2.5 mm.

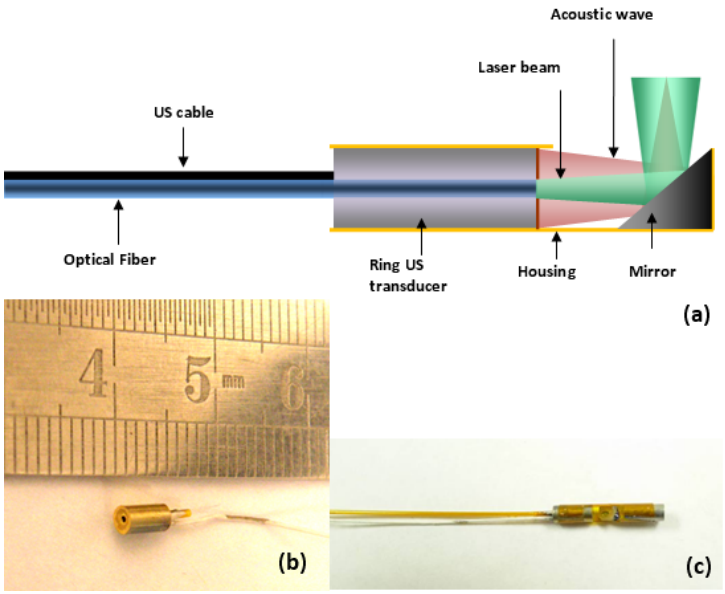

Figure 2: (a) Schematic of combined ultrasound and photoacoustic probe. (b) The photo of home-made ring shape ultrasound transducer. (c) The photo of the combined ultrasound and photoacoustic probe after packaging.

2.3 Tissue-mimicking phantom with inclusion and rabbit arota sample

In order to test the performance of the probe, first we obtain the combined ultrasound and photoacoustic imaging of the tissue-mimicking phantom. The phantom consisted of both optical and ultrasonic scattering background within an optical inclusion, and a air lumen of the contrast agent. The cylindrical phantom was made out of 10 wt% gelatin – as prepared. 2 wt% 0.5 – 15 micrometer silica dioxide powder was added as the ultrasonic scatterers and 10 vol% low-fat milk was added as the optical scatterers. As shown in Fig. 3, a 5 mm diameter hole was drilled in the center of the phantom and acted as the lumen of tissue. A 0.5 mm diameter graphite rod, working as the optical inclusion, was embedded in the phantom with the distance 3.5 mm from the center. By drilling the phantom, we created a 0.5 mm diameter air lumen, same dimension as the graphite rod, which appeared as an air bubble in the scanning cross-section. The tiny air lumen was 5 mm from the center and acted as the optical contrast agent.

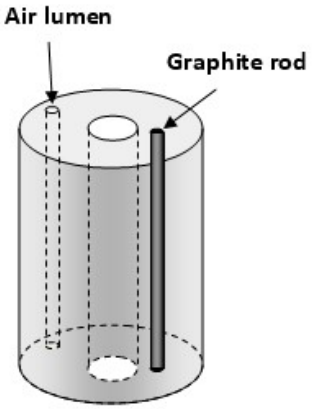

Figure 3 The 3-D schematic of the phantom with 0.5 mm diameter graphite rod and 0.5 mm diameter air lumen embeding in it.

In order to demonstrate the imaging ability of this dual-modality system, a section of normal rabbit aorta was prepared. For fixation, the aorta (only vascular) was immersed in 10% formalin for 24 hours, and then preserved in phosphate buffer. The aorta was pinned to a piece of cork and immersed in saline during the experiment.

3. RESULT AND DISCUSSION

3.1 Tissue-mimmicking phantom images

The result of combined ultrasonic and photoacoustic imaging of the tissue-mimicking phantom are presented in Fig.4. Both images in Fig.4 are displayed covering a 13 mm diameter field of view, i.e., each image has a radius of 6.5 mm. These two images were obtained from the same cross-section of the phantom.

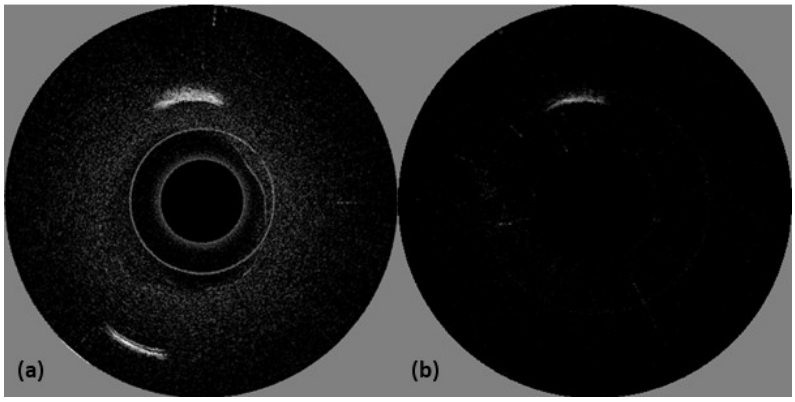

Figure 4: The cross-sectional (a)ultrasound , (b) photoacoustic image of the phantom. The field of view is 6.5 mm in radius in both images.

Fig.4 (a) is the ultrasound image which has the general structure of the phantom with two ultrasonic inclusions at 12 o'clock position and 7 o'clock position. One is graphite rod, the other one is air lumen. Aside from locating at different depth, it is hard to distinguish the two inclusions from each other by looking at the pattern of ultrasound imaging. Both inclusions have relatively different impedance from the surrounding tissues, so both of them appeared hyperechoic. However, air bubble is not rare, especially in some biological tissues. In this case, the ability to show the specificity and the contrast within a tissue sample is required. Photoacoustic images shown in Fig.4(b) illustrate the system's ability to provide optical contrast within the tissue. The reflective area located at 12 o'clock position in the image is the graphite rod, which matches the illustration in Fig.3. On the other hand, we can conclude that the 7 o'clock position is the image of the air bubble by comparing the Fig.4(a) and 4(b). By combining the two imaging modality together, the relative area of the inclusion and the whole tissue structure can be displayed and recognized. The complementary imaging of the ultrasound and photoacoustic illustrate the synergism of the combined system design.

3.2 Rabbit aorta images

In vitro imaging of a normal rabbit aorta was performed using the dual-modality probe to demonstrate the imaging ability, as shown in Fig.5. It is clear that the ultrasound imaging provides a full-depth cross-section image of the aorta displayed in Fig. 5(a). Fig. 5(b) is the photoacoustic image from the same cross section of the aorta. The photoacoustic image shows a maximum imaging depth of ~0.8 mm corresponding to the

ultrasound image. Moreover, as shown in Fig. 5(c), the similar shapes of ultrasonic and photoacoustic images indicate the superiority of the coaxial probe design in obtaining the co-registered images.

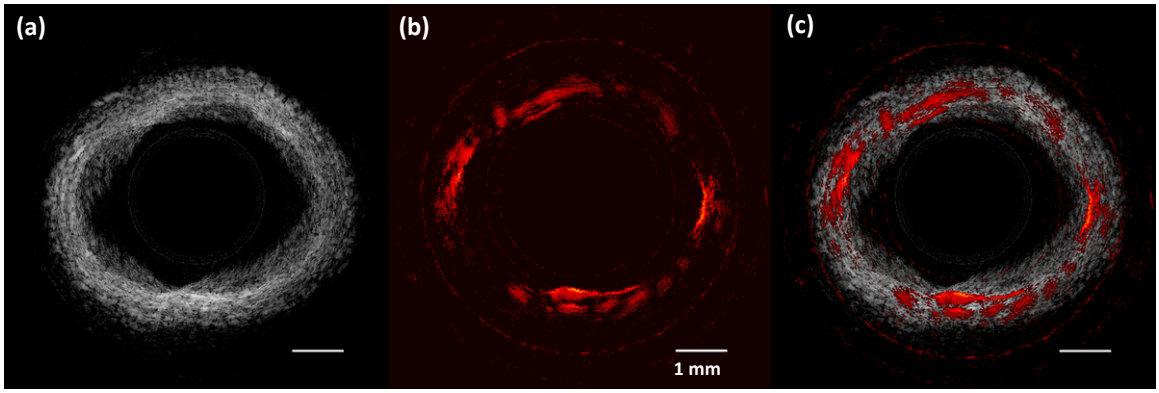

Figure 5: Cross-sectional (a)ultrasound, (b)photoacoustic and (c) combined images of a normal rabbit aorta.

4. CONCLUSION

We have presented a miniaturized imaging probe combining ultrasound and photoacoustic. The probe is formed by integrating a 40 MHz ring shape ultrasound transducer, a coaxial optical fiber, and a mirror. By imaging a graphite rod, the performance of the probe was tested. The coaxial design of the probe provided co-registered ultrasound and photoacoustic images of a normal rabbit aorta, which demonstrated the imaging ability of the dual-modality system.

ACKNOWLEDGMENT

We would like to thank Ms. Hongrui Li for preparing the tissue. This work is based on research supported by the NIH (CA-91717, EB-00293, EB10090, RR-01192) and the U.S. Air Force Office of Scientific Research, Medical Free-Electron Laser Program FA9550-08-1-0384. Mr. Xiang Li and Mr. Wei Wei have equal contributions to this paper and should be treated as co-first authors.

REFERENCES

[1] L. V. Wang, ed., *Photoacoustic Imaging and Spectroscopy* (Taylor & Francis/CRC Press, 2009).
[2] A. A. Oraevsky and A. A. Karabutov, in *Biomedical Photonics Handbook,* T. Vo-Dinh, ed.(CRC Press, 2003)
[3] L. V. Wang, "Multiscale photoacoustic microscopy and computed tomography," Nat. Photonics 3(9), pp. 503-509 (2009).
[4] M. Xu, L. V. Wang, "Photoacoustic imaging in biomedicine," Rev. Sci. Instrum. 77, pp. 041101-(1-22) (2006).
[5] C. Li, L. V. Wang, A. Aguirre, J. Gamelin, A. Maurudis, and Q. Zhu, "Real-time photoacoustic tomography of cortical hemodynamics in small animals," Journal of Biomedical Optics 15, 010509 (Feb. 16, 2010).
[6] Hu, K. Maslov and L. V. Wang, "Noninvasive label-free imaging of microhemodynamics by optical-resolution photoacoustic microscopy," Optics Express 17(9), 7688-7693 (Apr. 2009).

[7] G. Ku, K. Maslov, L. Li, and L. V. Wang, "Photoacoustic microscopy with 2-μm transverse resolution," Journal of Biomedical Optics 15, 021302 (Mar. 25, 2010).
[8] B. Rao, L. Li, K. I. Maslov, and L. V. Wang, "Hybrid-scanning optical-resolution photoacoustic microscopy system for in vivo vasculature imaging," Optics Letters 35 (10), 1521–1523 (May 2010).
[9] J.-M. Yang, K. Maslov, H.-C. Yang, Q. Zhou, L. V. Wang, "Endoscopic photoacoustic microscopy," Proc. SPIE 7177, 71770N (2009).
[10] J.-M. Yang, K. Maslov, H.-C. Yang, Q. Zhou, K. K. Shung, L. V. Wang, "Photoacoustic endoscopic," Optics Letters 34 (10), 1591-1593 (May 2009).
[11] S. Sethuraman, S. R. Aglyamov, J. H. Amirian, R. W. Smalling, and S. Y. Emelianov, IEEE Trans. Ultrason. Ferroelectr. Freq. Control 54, 978 (2007).